3D Separation

2D separation: at $\tau_w = \mu u_y = 0$ entire BL breaks away surface and must travel over separation bubble and into wake

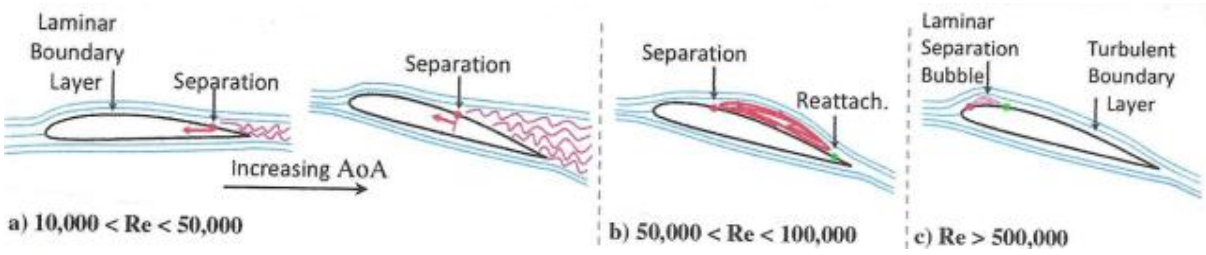

3D separation leads to more freedom and breakaway options and different types/definitions separations. For example: $\psi_\omega \to S$ while outer flow goes over separation bubble.

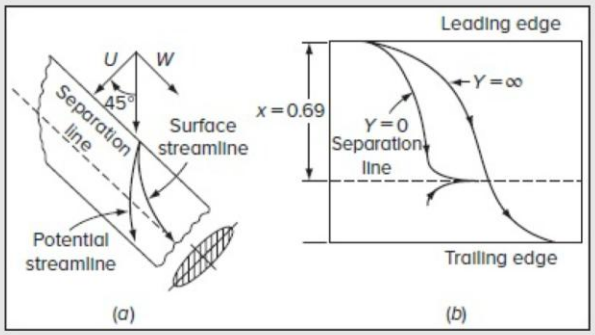

FIGURE 4-49

Two examples of outer potential flow and limiting surface streamlines for separating flow over an infinite yawed cylinder: (*a*) elliptical cylinder (1:6), ϕ = 45° [*after Wild* (*1949*)]; (*b*) $U = C(x - x_3)$, $W = W_0$ [*after Sears* (*1948*).]

According to active research in the mathematical topology of three-dimensional separation zones [Tobak and Peake (1982), Wang (1997)], four different points in separation can be distinguished:

1. *A nodal point*, where an infinite number of surface streamlines ("skin-friction lines") merge tangentially to the separation line.
2. *A saddle point*, where only two surface streamlines intersect and all others divert to either side.
3. *A focus*, or spiral node, which forms near a saddle point and around which an infinite number of surface streamlines swirl.
4. *A three-dimensional singular point*, not on the wall, where the velocity is zero, but serving as the center for a horseshoe vortex.

Singular Points

Singular points in the pattern of skin-friction lines occur at isolated points on the surface where the skin friction (τ_{w_1}, τ_{w_2}) in Equation (3), or alternatively the surface vorticity (ω_1, ω_2) in Equation (4), becomes identically zero. Singular points are classifiable into two main types: nodes and saddle points. Nodes may be further subdivided into two subclasses: nodal points and foci (of attachment or separation).

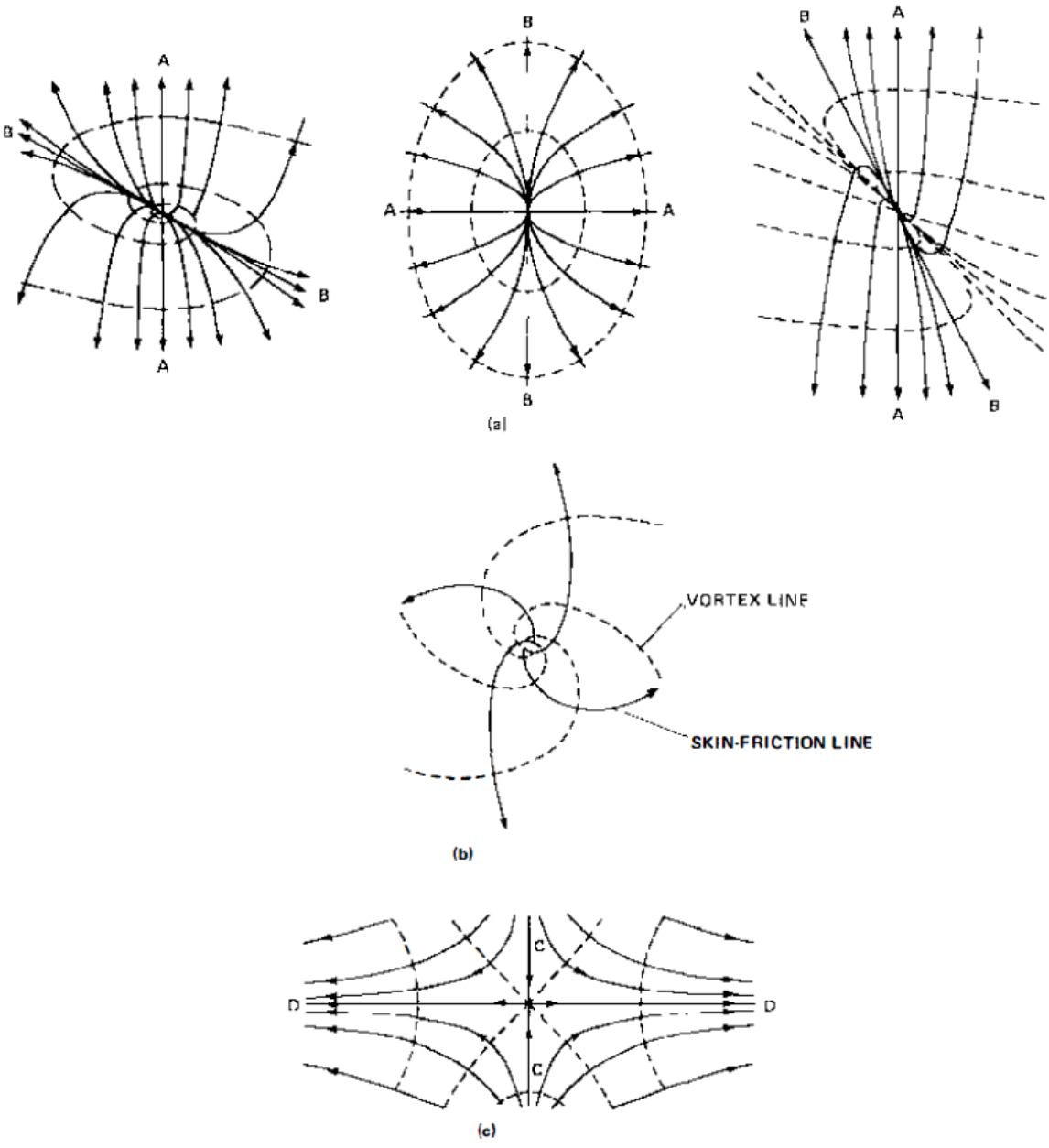

Figure 1 Singular points: (*a*) node; (*b*) focus; (*c*) saddle (Lighthill 1963).

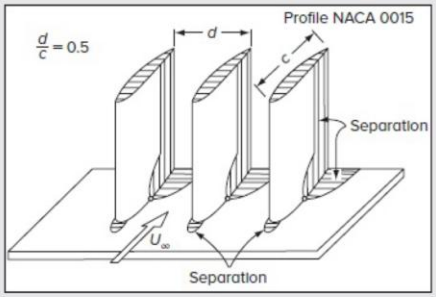

FIGURE 4-50
Separation regions in corner flow between airfoils. [*After Gersten* (*1959*).]

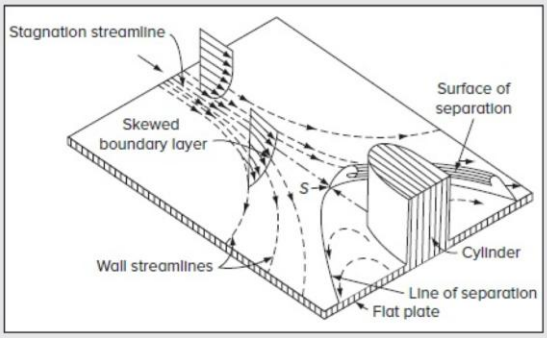

$p_x > 0 \Rightarrow$ junction/horseshoe vortex
S = nodal point of separation
other singular point of present

FIGURE 4-51
Three-dimensional separation in flat-plate flow against a cylindrical obstacle. [*After Johnston* (*1960*).]

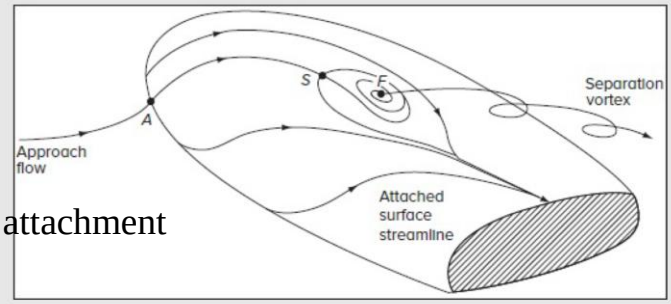

S = Saddle point
F = Focus point (near S)
= tornado vortex

nodal attachment point

FIGURE 4-52
Three-dimensional separation on a round-nosed body at an angle of attack, first described by Legendre (1965). Points *A*, *S*, and *F* represent a nodal attachment point, a saddle point, and a focus of separation point, respectively.

Closed separation: upstream flow does not enter separation region

Open separation: upstream flow may enter separation region

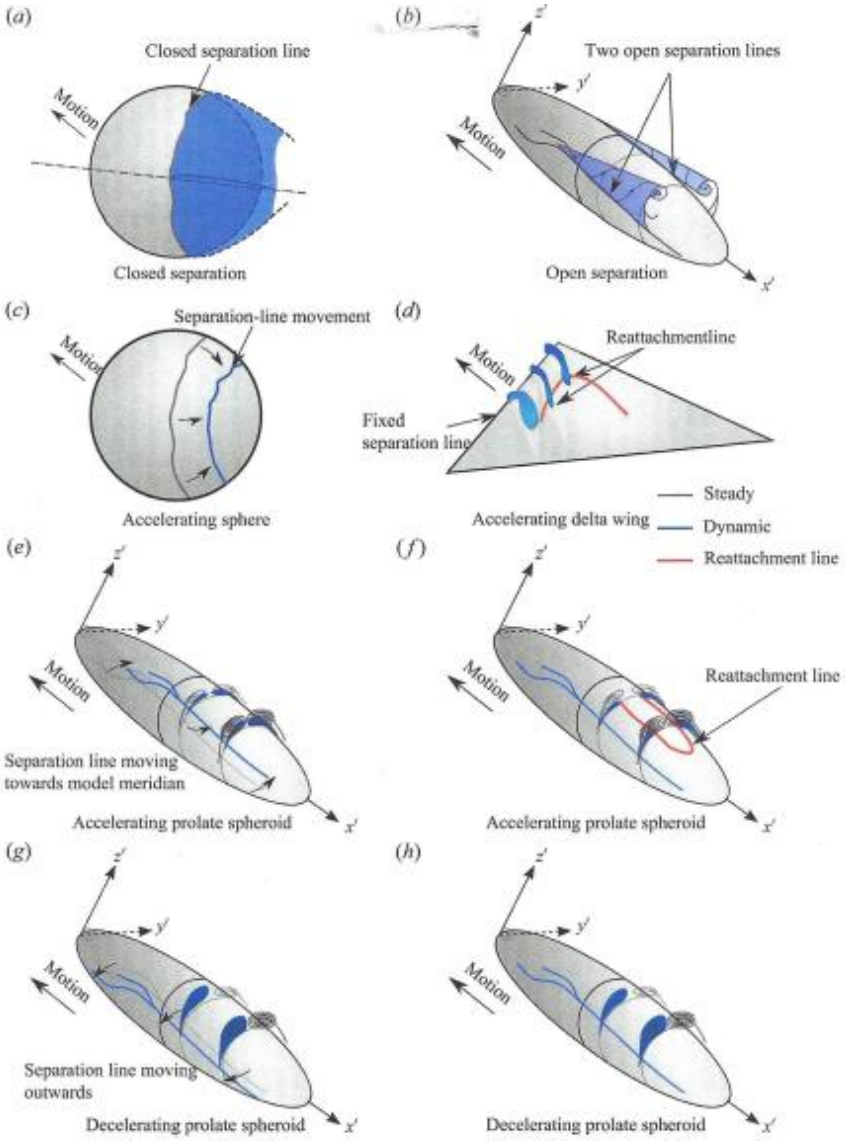

Figure 1. (*a*) Example of a closed separation with closed separation line. (*b*) A case with open separation with two open separation lines. (*c*) For an accelerating sphere, the separation line moves backwards in the subcritical Re range (Fernando *et al.* Reference Fernando, Marzanek, Bond and Rival2017). (*d*) For an accelerating delta wing, the flow has been observed to reattach on the wing surface (Marzanek & Rival Reference Marzanek and Rival2019). In contrast, for an accelerating prolate spheroid, a number of scenarios are possible: (*e*) the separation line will move closer to the model meridian centre or (*f*) a reattachment line will be created. Sketches in panels (*g*) and (*h*) illustrate possible scenarios for decelerations. To make the panels clear, the possible larger cross-flow separation for decelerations is only presented on one side of the model body.

Dynamic separation on an accelerating prolate spheroid, JFM: **22 November 2023**
Pengming Guo, Frieder Kaiser, David E. Rival

Unsteady Separation

Typical examples:

(1) start-up flow
(2) periodic flow

Chapter 3 Exact Solutions

$\underbrace{Stokes\ 1st \text{ and } 2\text{nd}}_{no\ separation}$

(a) Start-up flow circular cylinder. Stokes flow for low Re.

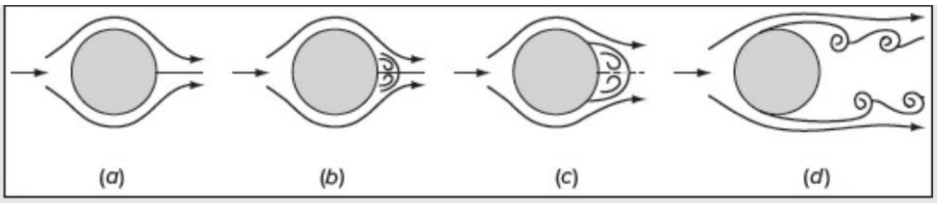

FIGURE 4-53

Start-up of viscous flow past a cylinder accelerated from rest: (*a*) Initial flow is nearly inviscid, resembling Fig. 1-4; (*b*) later, separation begins on the rear surface; (*c*) still later, separation extends up the rear surface in a symmetric vortex pattern; (*d*) finally, the double vortex becomes unstable, leading to an alternating Kármán vortex street, with the separation point on the front of the body.

(b) $\frac{Ut}{R} \approx 0.35$

(c) $\frac{Ut}{R} \approx 1.5$ strong symmetric vortex

(d) Kármán vortex street Strouhal number = fL/U ≈ 0.2

Moore, Rott, & Sears: MRS unsteady separation definition

Singular point $\left(x_s(t),\, y_s(t)\right)$ in the flow where $u_s = \frac{dx_s}{dt} = 0$ and $\tau_s = \omega_s = \frac{\partial u}{\partial y}|_s = 0$

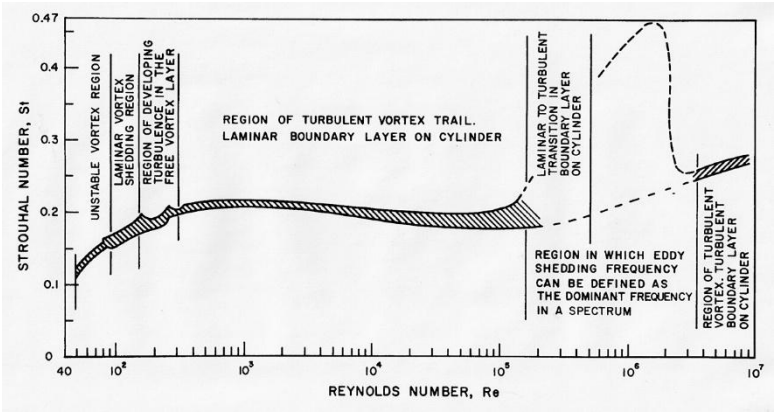

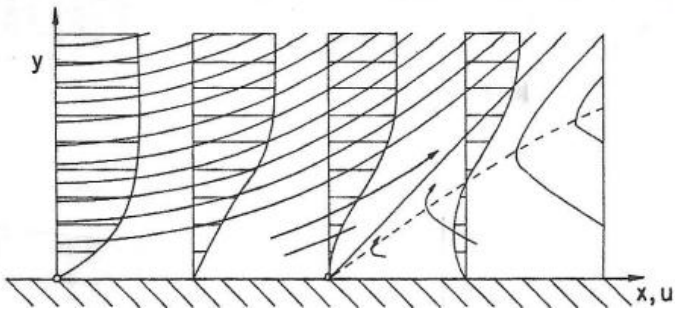

Fig. 7.1 Prandtl's sketch of the streamline pattern and velocity profiles in the neighborhood of separation.

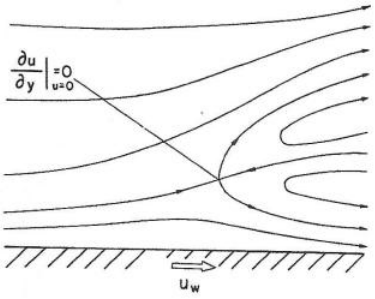

Fig. 7.2a Streamline pattern at a point of separation over a downstream moving wall.

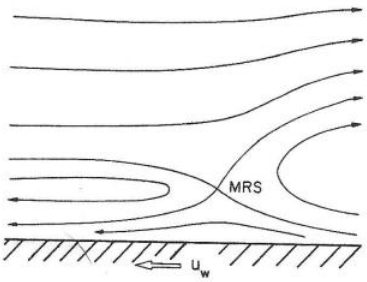

Fig. 7.2b Streamline pattern at a point of separation over an upstream moving wall.

Fig. 7.2c Velocity profiles corresponding to the pattern of Fig. 7.2a. The saddle point in Fig. 7.2a corresponds to the point $u = \partial u/\partial y = 0$ according to the MRS criterion.

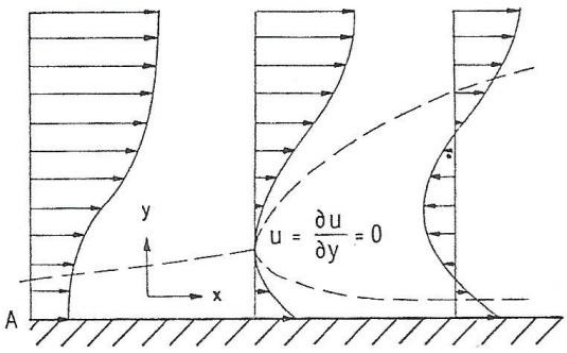

(2) periodic flows

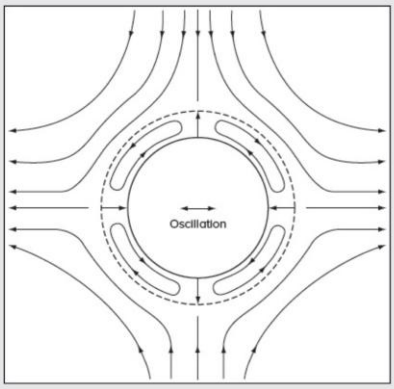

A<<L = length of body

FIGURE 4-54
Streamlines for acoustic streaming in the outer flow about an oscillating circular cylinder. [*After Schlichting* (1932).]

Assume body in uniform flow has potential flow $U_0(x)$ such that oscillating body motion creates

$$U(x,t) = U_0(x)\cos\omega t$$

relative body. Thus, BL driven by free stream similar Stokes 2nd. Schlichting series solution pp. 428–432: (0th order same Stokes 2nd)

0th order $u_0(x,t) = U_0(x)[\cos\omega t - e^{-\eta}\cos(\omega t - \eta)]$ $\quad \eta = y\sqrt{\frac{\omega}{2\nu}}$

2nd order includes steady-state term which does not vanish at large distances from the body

$\underbrace{u_2\left(x,\infty\right) = -\frac{3}{4}\frac{U_0}{\omega}U_{0_x}}_{\text{acoustic streaming}}$ due $u_0 u_{0_x}$ nonzero mean

acoustic streaming = steady-state motion towards decreasing $U_0(x)$ due body motion

Explains dust patterns Kundt tube

Periodic motions induce non-zero mean convection important stability and turbulence

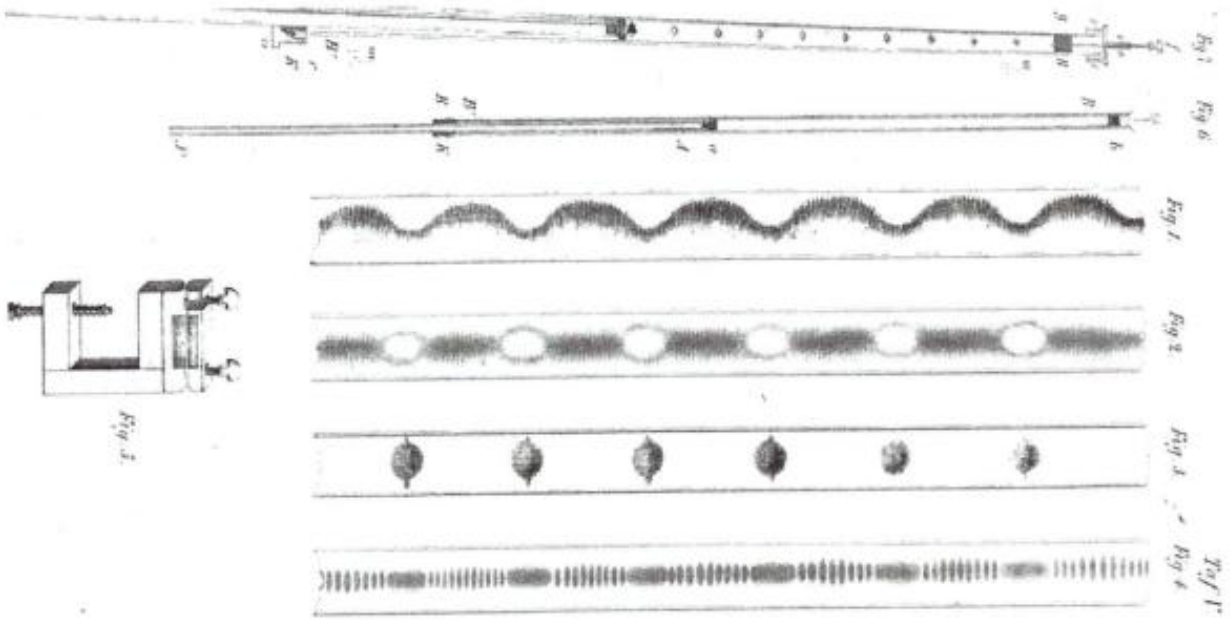

Kundt's tube is an experimental acoustical apparatus invented in 1866 by German physicist August Kundt[1][2] for the measurement of the speed of sound in a gas or a solid rod. The experiment is still taught today due to its ability to demonstrate longitudinal waves in a gas (which can often be difficult to visualise). It is used today only for demonstrating standing waves and acoustical forces.

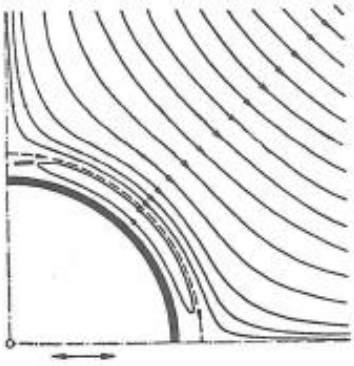

Fig. 15.7. Pattern of streamlines of the steady secondary motion in the neighbourhood of an oscillating circular cylinder

Fig. 15.8. Secondary flow in the neighbourhood of an oscillating circular cylinder. The camera moves with the cylinder. The metallic particles which serve to render the flow visible show up as wide bands owing to the long exposure time and to their reciprocating motion, after Schlichting [44]

3D Separation Patterns

Classification flow patterns for separation first approached using special planes curved or flat: body surface, symmetry, cross flow, or other.

2D vector field $u = \frac{dx}{dt}$ and $v = \frac{dy}{dt}$ has trajectory y(x) ⇒ flow patterns. On body surface ⇒ surface streamlines, i.e., shear stress lines. Patterns depend on motion of observer in unsteady flow. Not true vortex lines for translation, which are $\perp$ ψ on body surface. Assuming $\underline{u}$ continuous ⇒ trajectories and critical points = points $\underline{u}$ and $\underline{\omega} = 0$ and trajectories may split.

Theory and nomenclature from phase plane analysis of autonomous differential equations, e.g., Tobak and Peak (1982).

At critical points $\underline{u} = 0$ but derivative organized by:

(1) J = Jacobian $= u_x v_y - u_y v_x$

(2) $\Delta =$ divergence $= u_x + v_y$ plane of interest where $\Delta = -\omega_z$ and z normal to the plane

Thus, on body surface $\Delta = 0$.

In 3D invariant of strain tensor also investigated.

Critical points classified three groups depending on J and Δ.

(1) foci within area above parabola $J = \frac{\Delta^2}{4}$

(2) nodes between $J = \frac{\Delta^2}{4}$ and Δ axis

(3) saddles below Δ axis

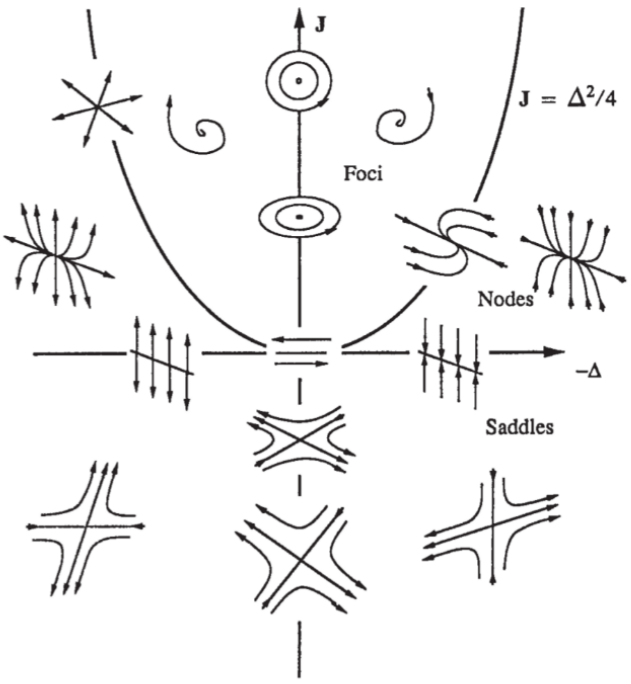

Figure 20.35 Types of critical points.

On boundary called focal or saddle node, and special case attachment saddle node = plane stagnation line, whereas special case attachment focus node = axisymmetric stagnation point.

2nd quadrant patterns are unstable since all trajectories leave these points and integration $u(t), v(t)$ from these points not possible.

1st quadrant patterns are stable since integration progresses towards these points.

$LHS = RHS$ figure except flow direction reversed

Critical points follow certain topological rules, e.g., on closed body $\#\text{nodes} - \#\text{saddles} = 2$, as per W2025 JBC test case.

Other special features: local separation lines, limit cycle lines or bifurcation lines (different nomenclature used).

Lines towards which other lines asymptote.

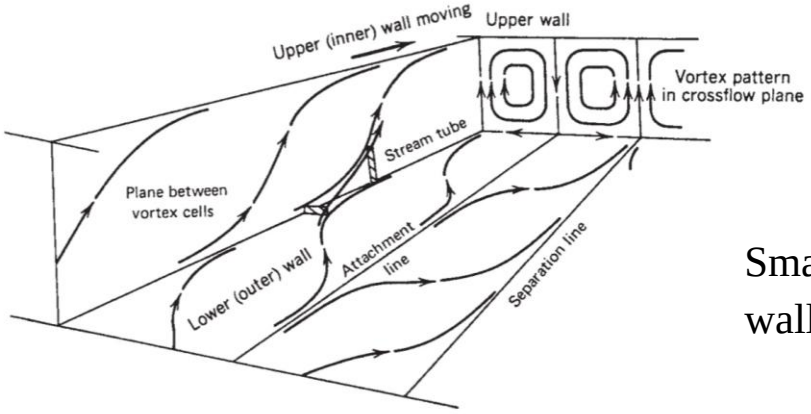

Small section outer wall

Figure 20.36 Streamlines in a Taylor vortex cell of a Couette flow. The wall and the surfaces separating vortex cells intersect in lines of separation and lines of attachment.

Taylor–Couette flow = stack spiral vortex cells due moving inner and stationary outer walls. Cross plane shows swirling vortices and wall shows lines of separation and attachment to which the streamlines asymptote.

In general, separation flow patterns are extremely complex and different analysis including alternative interpretations even for steady, much less unsteady flows.

Since separation usually unsteady, instability analysis such as shear layer, Kármán shedding, breathing mode, etc., often more productive.

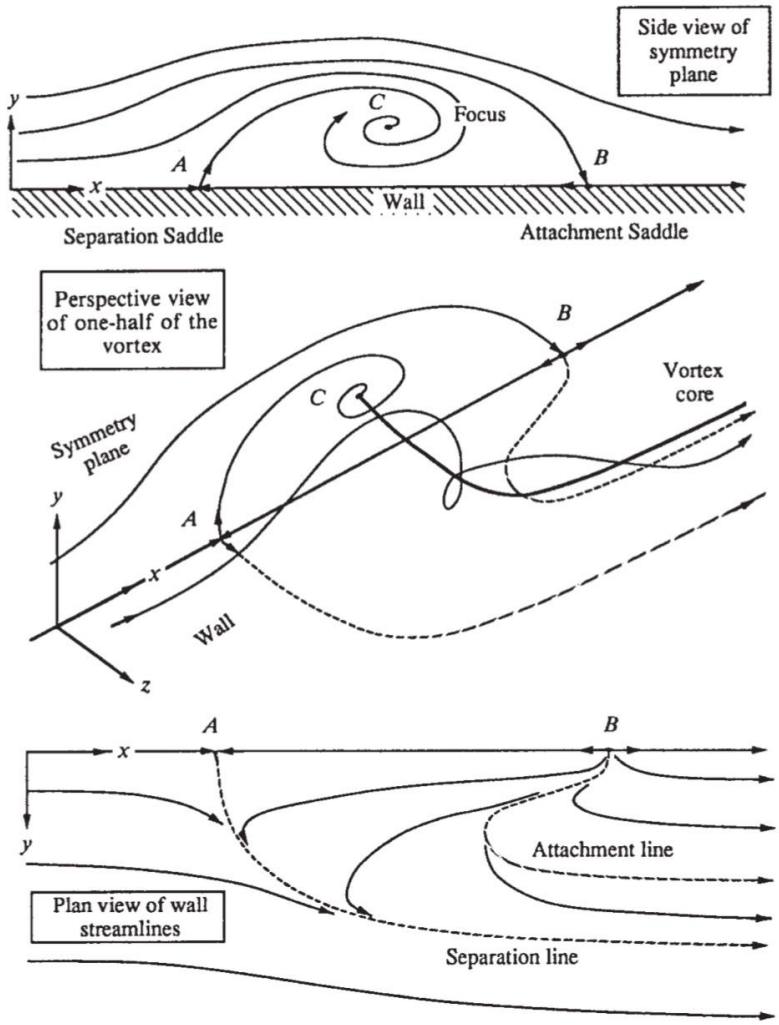

Figure 20.37 Separation pattern of a horseshoe vortex above a wall.

We see in Fig. 20.37 one of the simplest examples of a three-dimensional separation, a steady horseshoe vortex above a solid wall. The wall is in the $x-z$ plane, and only one-half the flow is shown because of symmetry. The vortex is perpendicular to the oncoming stream at point C, a spiral focus. Point A is a separation saddle point and point B is the attachment saddle point. A bifurcation line leaves A and proceeds to bend back along the wall. At some position the line ceases to be an asymptote and becomes an ordinary wall streamline. In a similar fashion, a bifurcation attachment line is emanating from B, and it could also turn into an ordinary streamline. The ultimate fate of the vortex is not depicted. In a very viscous flow, the vortex could die out downstream and only a uniform shear flow would remain.

Ann. Rev. Fluid Mech. 1982. 14:61-85

TOPOLOGY OF THREE-DIMENSIONAL SEPARATED FLOWS[1]

Murray Tobak and David J. Peake

National Aeronautics and Space Administration, Ames Research Center, Moffett Field, California 94035

INTRODUCTION

Three-dimensional separated flow represents a domain of fluid mechanics of great practical interest that is, as yet, beyond the reach of definitive theoretical analysis or numerical computation. At present, our understanding of three-dimensional flow separation rests principally on observations drawn from experimental studies utilizing flow visualization techniques. Particularly useful in this regard has been the oil-streak technique for making visible the patterns of skin-friction lines on the surfaces of wind-tunnel models (Maltby 1962). It is a common observation among students of these patterns that a necessary condition for the occurrence of flow separation is the convergence of oil-streak lines onto a particular line. Whether this is also a sufficient condition is a matter of current debate. The requirement to make sense of these patterns within a governing hypothesis of sufficient precision to yield a convincing description of three-dimensional flow separation has inspired the efforts of a number of investigators. Of the numerous attempts, however, few of the contending arguments lend themselves to a precise mathematical formulation. Here, we shall single out for special attention the hypothesis proposed by Legendre (1956) as being one capable of providing a mathematical framework of considerable depth.

Legendre (1956) proposed that a pattern of streamlines immediately adjacent to the surface (in his terminology, "wall streamlines") be considered as trajectories having properties consistent with those of a continuous vector field, the principal one being that through any regular (nonsingular) point there must pass one and only one trajectory. On the basis of this postulate, it follows that the elementary singular points of the field can be categorized mathematically. Thus, the types of singular points, their number, and the rules governing the relations between them can be said to characterize the pattern. Flow separation in this view has been defined by the convergence of wall streamlines onto a particular wall streamline that originates from a singular point of particular type, the saddle point. We should note, however, that this view of flow separation is not universally accepted, and, indeed, situations exist where it appears that a more nuanced description of flow separation may be required.

Lighthill (1963), addressing himself specifically to viscous flows, clarified a number of important issues by tying the postulate of a continuous vector field to the pattern of skin-friction lines rather than to streamlines lying just above the surface. Parallel to Legendre's definition, convergence of skin-friction lines onto a particular skin-friction line originating from a saddle point was defined here as the necessary condition for flow separation. More recently, Hunt et al. (1978) have shown that the notions of elementary singular points and the rules that they obey can be easily extended to apply to the flow above the surface on planes of symmetry, on projections of conical flows (Smith 1969), on crossflow planes, etc. (see also Perry & Fairlie 1974). Further applications and extensions can be found in the various contributions of Legendre (1965, 1972, 1977), Oswatitsch (1980), and in the review articles by Tobak & Peake (1979) and Peake & Tobak (1980).

As Legendre (1977) himself has noted, his hypothesis was but a reinvention within a narrower framework of the extraordinarily fruitful line of research initiated by Poincaré (1928) under the title, "On the Curves Defined by Differential Equations." Yet another branch of the same line has been the research begun by Andronov and his colleagues (1971, 1973) on the qualitative theory of differential equations, within which the useful notions of "topological structure" and "structural stability" were introduced. Finally, from the same line stems the rapidly expanding field known as "bifurcation theory" (see the comprehensive review of Sattinger 1980). Applications to hydrodynamics are exemplified by the works of Joseph (1976) and Benjamin (1978). It has become clear that our understanding of three-dimensional separated flow may be deepened by placing Legendre's hypothesis within a framework broad enough to include the notions of topological structure, structural stability, and bifurcation. Bearing in mind that we still await a convincing description of three-dimensional flow separation, we may ask whether the broader framework will facilitate the emergence of such a description. In the following, we shall try to answer this question, limiting our attention to three-dimensional viscous flows that are steady in the mean.

Free-Surface Wave-Induced Separation

Z. J. Zhang[1]
Graduate Research Assistant.

F. Stern
Professor.

Department of Mechanical Engineering,
Iowa Institute of Hydraulic Research,
The University of Iowa,
Iowa City, Iowa 52242

Free-surface wave-induced separation is studied for a surface-piercing NACA 0024 foil over a range of Froude numbers (0, .2, .37, .55) through computational fluid dynamics of the unsteady Reynolds-averaged Navier-Stokes and the continuity equations with the Baldwin-Lomax turbulence model, exact nonlinear kinematic and approximate dynamic free-surface boundary conditions, and a body/free-surface conforming grid. The flow conditions and uncertainty analysis are discussed. A topological rule for a surface-piercing body is derived and verified. Steady-flow results are presented and analyzed with regard to the wave and viscous flow and the nature of the separation.

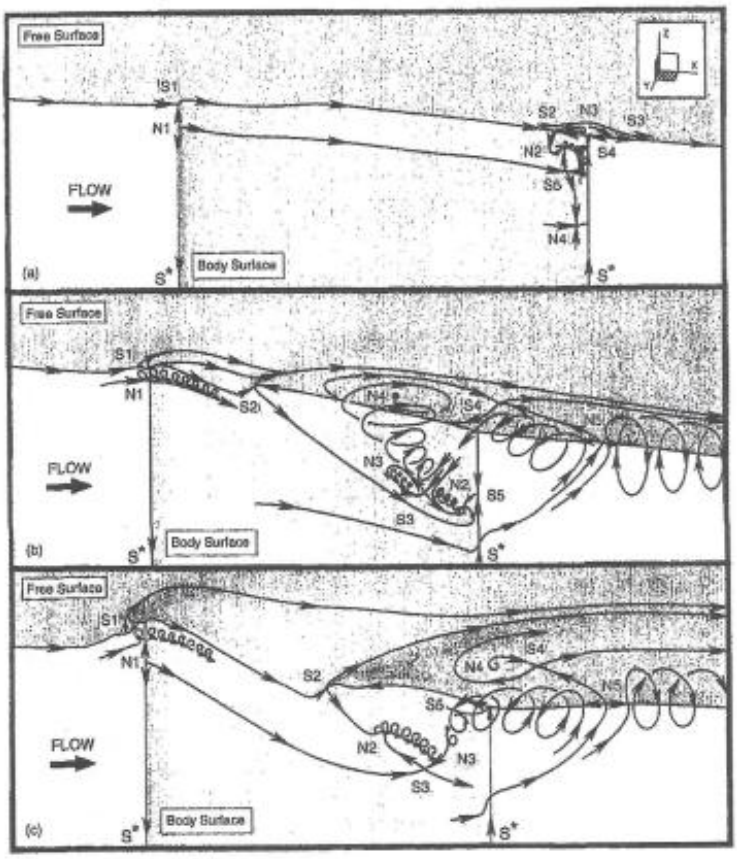

Fig. 9 Topological structures: (*a*) Fr = 0.20, (*b*) Fr = 0.37, and (*c*) Fr = 0.55